New Enkephalin Nanomedicines for Pain Alleviation, Overcoming the Side Effects of Morphine

Sinda Lepetre-Mouelhi, Jiao Feng, and Patrick Couvreur

Abstract Over the last years, the nanomedicines has been recognized as a key element, capable of providing new and innovative medical solution to address unmet medical needs. More specifically, Squalene-based nanoparticles have opened exciting perspectives for drug delivery due to their biodegradability and their non-toxicity. In this study, it was shown for the first time, that the rapidly metabolized Leu-enkephalin (LENK) neuropeptide, once conjugated to the biocompatible lipid squalene (SQ) and formulated into nanoparticles, may become pharmacologically efficient. First, the resulting LENK-SQ bioconjugates were synthesized using different biocleavable chemical linkers, in order to modulate the LENK release from their formulation into nanoparticles (NPs). This nanoformulation led to new nanosystems exhibiting high drug loadings, allowed an efficient protection to LENK from early metabolism and conferred to the released neuropeptide a significant anti-hyperalgesic effect in a rat model of inflammatory pain which lasted longer than after treatment with morphine. A biodistribution study, as well as, the use of brain-permeant and -impermeant opioid receptor antagonists indicated that LENK-SQ NPs acted exclusively through peripherally located opioid receptors. This study showed that LENK-SQ bioconjugates may be beneficial in impacting the opioid crisis as these LENK-SQ NPs (i) exhibited higher affinity toward δ-opioid receptors versus μ-opioid receptors, (ii) showed exclusively peripheral activity (no BBB penetration) so no CNS addiction and (iii) took advantage of the inflammatory process to optimize drug concentrations at the site of injury.

Keywords Nanomedicine · Leu-Enkephalin · Squalene · Prodrug · Bioconjugate · Hyperalgesia · Inflammatory pain · Opioid receptors · Peripheral effect · Rat

S. Lepetre-Mouelhi (✉) · J. Feng · P. Couvreur
Institut Galien Paris-Sud, UMR8612, Université Paris-Saclay,
92290 Châtenay-Malabry, France
e-mail: sinda.lepetre@universite-paris-saclay.fr

M. J. M. Abadie et al. (eds.), *New Trends in Macromolecular and Supramolecular Chemistry for Biological Applications*, https://doi.org/10.1007/978-3-030-57456-7_10

1 Introduction and State-of-Art on Nanomedicines

Conventional chemotherapy is often hampered by poor diffusion through biological barriers such as epithelium, endothelium, cell membranes, and a rapid metabolization and clearance from the body. In addition, it frequently leads to a non-specific biodistribution of the drug in the body thus generating severe side effects due to drug losses in healthy organs and tissues.

To circumvent these drawbacks, the drug can be encapsulated into **nanoparticles** (NPs). This nanoparticular formulation allows protection to the drug from degradation, an efficient targeting towards diseased tissues, a better intracellular diffusion and a controlled release (Peer et al. 2007; Wang et al. 2012). A nanoparticle is composed of a core surrounded by a corona. Typically, the **core** material encapsulates the drug. It can be made of organic or inorganic compounds from natural and synthetic sources, such as polymeric materials, lipids, metal oxides, etc.… The **corona**, for its part, is a natural protein layer spontaneously formed around nanoparticles when exposed to biological media. The corona is constituted of plasma proteins, such as Albumin, immunoglobulin G (IgG), fibrinogen, apolipoproteins, coagulation factors, complement proteins… The formation of the protein corona around nanoparticles is dependent on physico-chemical properties of NPs including nanoparticle size, surface charge, hydrophobicity, surface chemistry and is characteristic of the environment in which are dispersed NPs. The corona can also be synthetic when designed to (i) confer stealth properties to the nanoparticle against immune system or (ii) enhance their targeting ability. In the first case, the corona is composed of Polyethylene Glycol (PEG) chains covalently linked or adsorbed onto the surface of the NP in order to prevent interactions between the particle surface and the plasma proteins (thus avoiding recognition by reticuloendothelial system). In the second case, for a better targeting, the corona may be constituted of PEG-chains grafted to specific ligands or only specific ligands adsorbed on the surface of the nanoparticle. The corona affects the fate of the nanoparticle in the body. It determines the rate of clearance from the bloodstream, the volume of distribution, the organ disposition, and the rate and route of clearance from the body.

These drug delivery nanosystems may be classified in 2 categories: organic NPs (e.g., polymeric, liposomes, micelles, etc.) and inorganic NPs (e.g., gold, silica, iron oxide, etc.).

Currently, there are a number of nanomedicines that have been approved for clinical use, either by the Food and Drug Administration (FDA) in the United States (51 FDA-approved nanomedicines), or the European Medicines Agency (EMA) in the European Union and more than 77 nanomedicines are in clinical trials (Bobo et al. 2016) (Anselmo and Mitragotri 2016). Among FDA-approved nanomedicines, most of organic NPs are liposomal systems and are mainly used in cancer therapy. The first approved nanomedicine was Doxil (FDA 1995), encapsulating the doxorubicin for cancer treatment (Barenholz and (Chezy) 2012). Then, other liposomes were also developed such as DaunoXome (daunorubicin), Myocet (doxorubicin), Marqibo (vincristine) and most recently, Onivyde (irinotecan) (Fox 1995; Leonard et al.

Leonard et al. 2009; Silverman et al. 2013; Carnevale and Ko 2016). The majority of these formulations are not PEGylated, with the exception of Doxil and Onivyde (Chang et al. 2015). Vyxeos is the first clinically approved liposome to deliver a synergistic combination of 2 drugs, daunorubicin and cytarabine for the treatment of acute myeloid leukemia in August of 2017 (Krauss et al. 2019). All of these nanoformulations are passively targeted with the ability to preferentially accumulate at tumor sites via the enhanced permeation and retention (EPR) effect (Maeda 2012). The liposomes are also used in some others clinical applications, such as general anesthesy with Diprivan (Cummings et al. 1984; Thompson and Goodale 2000). The FDA-approved Visudyne, a light-activated liposome loading verteporfin, was used in photodynamic therapy for choroidal neovascularization due to age-related macular degeneration (Schmidt-Erfurth and Hasan 2000). For the treatment of some bacterial/fungal infections, liposomes loading amphotericin B (AmBisome) have been clinically approved as well as lipid-complexed formulations, such as Abelcet and Amphotec (Hamill 2013; Rust and Jameson 1998). Two other liposomes Inflexal V and Epaxal were commercialized successfully as vaccines. These virosome-based vaccines incorporated inactivated influenza and hepatitis A virus respectively (Fan et al. 2021). It should be noted that the virosomes Inflexal V and Epaxal have since been phased out of the clinic. Other non liposomal organic nanoformulations were also approved. Abraxan, is a protein nanoparticle which is used in cancer therapy with paclitaxel formulated as albumin bound (Tomao et al. 2009). Polymeric nanoparticles were also used, such as Copaxone as immunomodulator, Neulatsa for chemotherapy induced neutropenia, Cimzia for the treatment of several autoimmune diseases, Plegridy treating relapsing multiple sclerosis and adynovate for the treatment of hemophilia A (Bobo et al. 2016). In the past few years, lipid nanoparticles have emerged as one of the most advanced and efficient mRNA delivery platforms. In that respect, the lipid nanoparticles Onpattro (Patisiran) delivering siRNA for the silencing of a specific gene responsible for expression of transthyretin (causing hereditary transthyretin amyloidosis), were recently approved (2018) (Adams et al. 2018). In 2020, an effective vaccine against the severe acute respiratory syndrome coronavirus 2 (SARS-CoV-2) (which emerged in late 2019) was approved (Jackson et al. 2020). The candidate vaccine mRNA-1273 is a lipid nanoparticle encapsulating a nucleoside-modified messenger RNA (mRNA) that encodes the SARS-CoV-2 spike (S) glycoprotein. Hence, approval of the first vaccine using lipid nanoparticles, highly effective against the devastating SARS-CoV-2 pandemic represents a major milestone for nanomedicines.

Approved inorganic NPs, for their part, are mainly iron-based colloids. They are used as iron-replacement therapies for treatment of anemia, such as Cosmofer, Dexferrum, Ferrlecit, Injectafter, in order to increase iron concentration in the body (Coyne and Auerbach 2010). They are also widely used as contrast agents for Magnetic Resonance Imaging (MRI) for imaging a variety of cancers and pathologies (Gupta and Gupta 2005; Wang et al. 2001; Na et al. 2009; Laurent et al. 2008). Recently, BTXR3/Hensify a crystalline hafnium oxide nanoparticle with negatively charged phosphate coating, received aproval in 2019 (Bonvalot et al. 2019). These

inorganic nanoparticles enhances external radiotherapy via a physical mode of action that relies on hafnium's natural radioenhancing properties.

However, despite the large number of successful nanomedicines that have reached the market, further development of new nanoformulations is still urgently needed to address current global health challenges, which requires collaborative efforts of scientists arising from different disciplines. In this context, Couvreur's team developed a very promising nanomedicine plateform for the treatment of severe diseases, using natural and biocompatible materials such as squalene lipid.

2 The Squalenoylation Nanotechnology: An Innovative and Efficient Nanoformulation

Squalene (SQ), a natural endogenous lipid belonging to the chemical class of triterpenes, is formed by six isoprene units and is an intermediate metabolite in the synthesis of cholesterol. It is widely distributed in nature and with reasonable amounts found in shark liver oil, olive oil, wheat germ oil and rice bran oil. It received its name because of its occurrence in shark liver oil (Squalus spp.) (Miettinen and Vanhanen 1994). Because it is of biological origin and frequently used as a dietary supplement, SQ is favourably predisposed from a toxicological standpoint; thus, it has been extensively used as a carrier/adjuvant in therapeutic applications. «The squalenoylation nanotechnology» involves the linkage of a fonctionnalized SQ (squalenic acid, squalenol, squalenamine, SQ maleimide, etc.…) to therapeutic agents using a chemical biocleavable linkage, such as ester, amide, hydrazone, carbamate, disulfide, etc.… The resulting SQ based bioconjugates, which are prodrugs, are bioreversible derivatives that undergo an enzymatic and/or a chemical transformation *in vivo* to release the active drug. Owing to the rigid structural property of SQ, these SQ-drug bioconjugates may self-assemble spontaneously in aqueous solutions into nanoparticles without the use of any surfactant and with high drug loading. Since its first application in 2006, squalenoylation nanotechnology has showed great potential for the delivery of various therapeutic agents in a safer and more efficient manner. Indeed, this new concept offers various advantages in comparison with the conventional nanocarriers. Contrary to polymer nanoparticles or liposomes nanoformulations which encapsulate physically the drugs into their matrices, the squalene-drug conjugates NPs involve a chemical encapsulation approach, thus preventing the "burst" release phenomenon (Couvreur et al. 2006). The supramolecular organization of these NPs allows protection to the therapeutic agents from degradation/metabolization resulting in greater plasmatic half-life, while controlling and extending the drug release. Furthermore, these nanosystems facilitated drug's passage through biological membranes due to the lipophilic properties of SQ resulting in an enhanced drug concentration within targeted tissues and cells and generating significant increase in drug pharmacological activity. Proofs of this concept have been established with drugs presenting different physicochemical characteristics, like

small hydrophilic or lipophilic molecules. Generally, the squalenoylation favorably modifies *in vivo* the pharmacokinetic profile and biodistribution of the carried drug, allowing its intravenous administration as NPs and increasing its therapeutic index (Desmaële et al. 2012; Feng et al. 2017). Thus, this drug delivery platform opened exciting perspectives in the drug delivery field. However, it has been a tremendous challenge to extend the SQ-based bioconjugation approach to molecules with higher molecular weight such as peptides, due to several obstacles in performing successful conjugation reactions. First, peptides are unstable biomolecules. Second, they are hydrophilic molecules, therefore, they have no affinity for lipophilic molecules such as squalene. In addition, the chemical modification of a peptide often results in a loss of its pharmacological activity. Thus, the chemical approach using squalenoylation nanotechnology has overcome all these hurdles, allowing the design of a small library of innovative neuropeptide-SQ bioconjugates for pain management. Thus, owing to a simple conjugation with the lipid squalene, the rapidly metabolized Leu-enkephalin (LENK) neuropeptide may become pharmacologically efficient.

3 Squalene-based Nanomedicines for Pain Management: Leu-Enkephalin-Squalene Nanoparticles (LENK-SQ NPs)

According to CDC/NCHS, National Vital Statistics System, every day, more than 115 people in the United States die after overdosing on opioids (Adams 2018). The misuse of and addiction to opioids, especially morphine, represents a serious national crisis in the US that affects public health, as well as, social and economic welfare. This highlights the need to urgently find new painkillers devoided of severe side effects. In this context, endogenous neuropeptides, such as enkephalins, are very promising painkillers which unlike morphin, exhibit a higher affinity towards delta-opioid receptors in comparison with mu (Janecka et al. 2004). This feature is of great importance since δ-opioid receptor ligands are believed to have a much lower abuse potential, as well as, reduced respiratory, gastrointestinal and cognitive disorders (Contet et al. 2004; Kiritsy-Roy et al. 1989; Abbadie and Abbadie 2002; Pasternak and Abbadie 2013; Tavani et al. 1990; Dykstra et al. 2002). However, because of pharmacokinetic issues, and rapid plasma metabolization, the enkephalins were not expoitable up to now.

4 Synthesis of Leu-Enkephalin-SQ Bioconjugates

In this context, in order to exploit its analgesic potential, the currently unusable Leu-enkephalin (LENK) neuropeptide was conjugated to the SQ derivative. Thus, various squalenoyl-Leu-enkephalin (LENK-SQ) conjugates were designed with

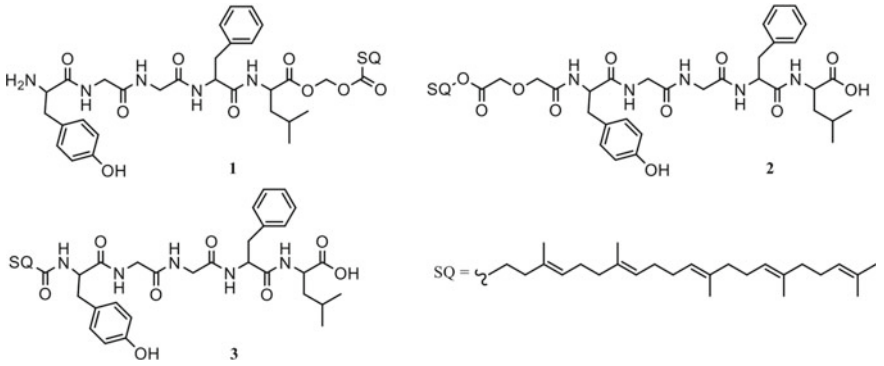

Fig. 1 Chemical structures of the bioconjugates. (1) Leu-enkephalin-squalene with dioxycarbonyl linker (LENK-SQ-Diox), (2) Leu-enkephalin-squalene with diglycolic linker (LENK-SQ-Dig), and (3) Leu-enkephalin-squalene with amide linker (LENK-SQ-Am). Figure reproduced from Ref. Feng et al. (2019), © 2019 AAAS

different chemical linkers using bioconjugation approach (Fig. 1). Therefore, LENK neuropeptide exhibits 2 potential sites for SQ conjugation: C-terminal acid and N-terminal amine. It must be emphasized that the N-terminal of LENK is required for binding to opioid receptors (Büscher et al. 1976). However, based on the fact that the amide bond is susceptible to be cleaved by overexpressed peptidases within inflammation site, (Viswanatha Swamy and Patil 2008) the conjugation on N-terminal was also achieved. Thus, a simple amide bond between SQ and LENK was first considered. Subsequently, two linkers with different sensitivity to hydrolysis were also used in order to modulate the release kinetics of LENK from NPs. Practically, conjugation of the squalenic acid (SQ derivative) on N-terminal LENK was performed through a simple amide bond (LENK-SQ-Am conjugate). Using diglycolic spacer, squalenol was also conjugated to N-terminal LENK (LENK-SQ-Dig conjugate) while through dioxycarbonyl linker the squalenic acid was coupled to C-terminal LENK (LENK-SQ-Diox conjugate).

The LENK-SQ-Diox conjugate was synthesized by alkylation of the carboxylate function of the peptide with the chloromethyl ester of squalenic acid, which resulted from the treatment of squalenic acid with chloromethyl chlorosulfate. Prior to react with the chloromethyl ester of squalenic acid, the LENK was protected by Alloc (allyloxycarbonyl) group on its N-terminal amine, in order to avoid N-terminal conjugation. Subsequent deprotection of Alloc-LENK-SQ under neutral conditions was then achieved by catalytic transfer hydrogenation method using triethylsilane and 10% Pd-C (Mandal and McMurray 2007), affording pure LENK-SQ-Diox in 9.5% yield (Fig. 2). The LENK-SQ-Dig prodrug was obtained from the conjugation between LENK and squalene diglycolic acid, activated by ethyl chloroformate. The squalene diglycolic acid resulted from a reaction between the squalenol and diglycolic anhydride. The LENK-SQ-Dig was obtained with 69% yield (Fig. 3). It was expected that the oxa moiety of the diglycolate linker enhances the susceptibility to hydrolysis by increasing the distance between LENK and SQ and so the accessibility

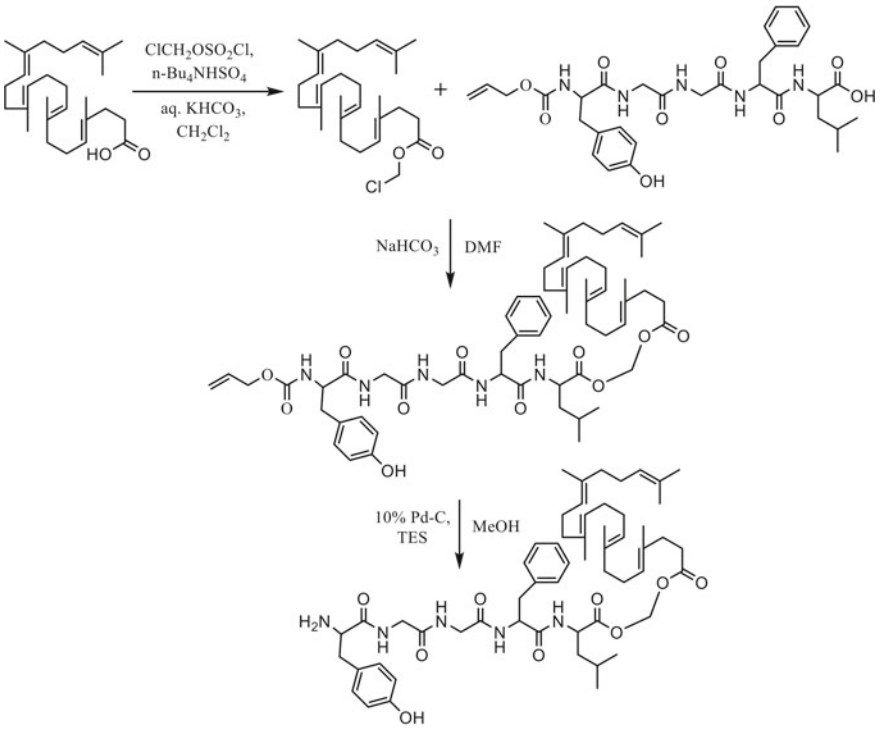

Fig. 2 Synthesis of Leu-enkephalin-squalene with dioxycarbonyl linker (LENK-SQ-Diox). Figure reproduced from Ref. Feng et al. (2019), © 2019 AAAS

to the linkage by enzymes. Direct conjugation between LENK and squalenic acid via amide bond was achieved by acid activation using ethyl chloroformate, affording LENK-SQ-Am in 73% yield (Fig. 4) (Feng et al. 2019).

It was expected that LENK-SQ-Diox released faster the LENK than LENK-SQ-Dig, and LENK-SQ-Am was supposed to trigger the slower release as reported in the literature (Sémiramoth et al. 2012).

5 LENK-SQ Nanomedicines: Preparation and Characterization

The LENK-SQ bioconjugates were then formulated as nanoparticles using simple nanoprecipitation technique without the aid of any surfactant. In that respect, LENK-SQ ethanolic solutions were nanoprecipitated in dextrose solution (2 mg/mL) and exhibited impressively high drug payloads (i.e. 53 to 59%) in comparison with conventional nanoparticles or liposomes which amounted to a maximum of 5% (Betageri et al. 1997; Chen et al. 2008). The size of the NPs varied from 61 to

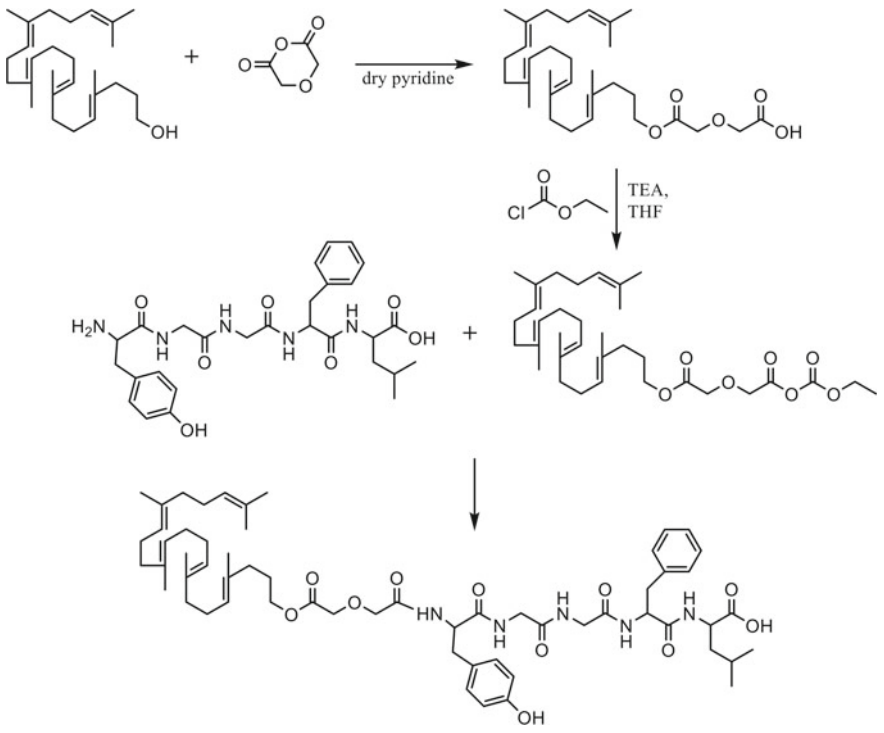

Fig. 3 Synthesis of Leu-enkephalin-squalene with diglycolic linker (LENK-SQ-Dig). Figure reproduced from Ref. Feng et al. (2019), © 2019 AAAS

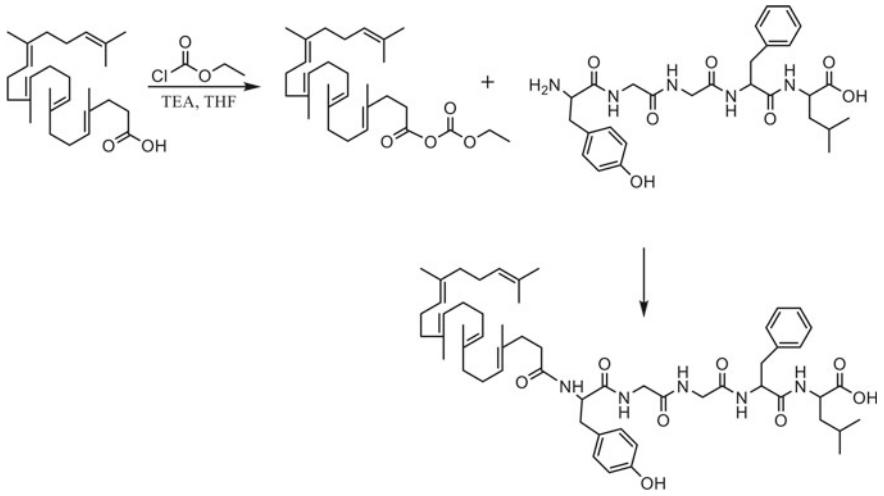

Fig. 4 Synthesis of Leu-enkephalin-squalene with amide linker (LENK-SQ-Am). Figure eproduced from Ref. Feng et al. (2019), © 2019 AAAS

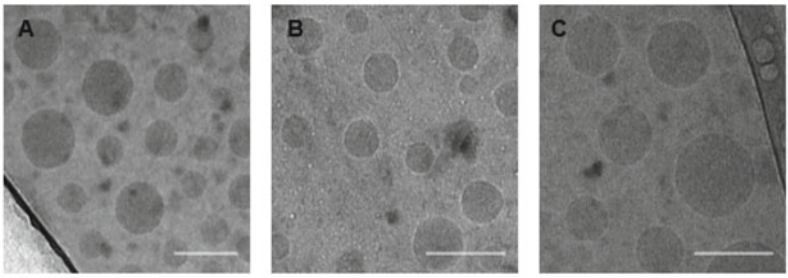

Compounds	Size (nm)	PDI	Zeta potential (mV)	Drug loading (%)
LENK-SQ-Diox	120±6	0.25±0.01	+33±4	57.38
LENK-SQ-Dig	75±11	0.13±0.05	-35±7	53.41
LENK-SQ-Am	122±22	0.08±0.01	-31±10	59.22

Fig. 5 NP characterization. Representative cryo-TEM images showing the formation of NPs from different bioconjugates: **A** LENK-SQ-Diox NPs, **B** LENK-SQ-Dig NPs, and **C** LENK-SQ-Am NPs. Scale bars, 100 nm. Physicochemical characteristics of NPs [i.e., size, polydispersity index (PDI), zeta potential, and % drug loading] are shown in the table. Figure reproduced from Ref. Feng et al. (2019), © 2019 AAAS

112 nm, depending on the conjugation site and also the linkage between SQ and enkephalin (Fig. 5). The NPs displayed spherical and monodisperse structures with net positive or negative surface charge (Fig. 5), which could be attributed to the free C- or N-terminal function of the peptide depending on the bioconjugation mode. Indeed, in case of the LENK-SQ-Diox bioconjugate, the net positive charge was due to free N-terminus site (primary amino group) of the bioconjugate, resulting from SQ conjugation on the C-terminus of LENK peptide. Conversely, the zeta potential became negative when the conjugation with SQ was performed on the N-terminus LENK peptide (LENK-SQ-Dig and LENK-SQ-Am). The sizes and the surface charges of the LENK-SQ NPs were found to be quite stable at +4 °C during several days (Feng et al. 2019).

6 *In vitro* Release Study of LENK from LENK-SQ Nanoparticles in Serum

The chemical stability of the different linkers (i.e., direct amide or dioxycarbonyl or diglycolate spacers) was studied after incubation of the LENK-SQ NPs with mouse serum in order to ascertain that free LENK peptide could be released from the LENK-SQ nanoparticles (Fig. 6). The study clearly showed that only LENK-SQ-Diox and LENK-SQ-Dig released the peptide. In the case of LENK-SQ-Diox NPs, the experiments highlighted the gradual decrease of bioconjugate concentration in favour

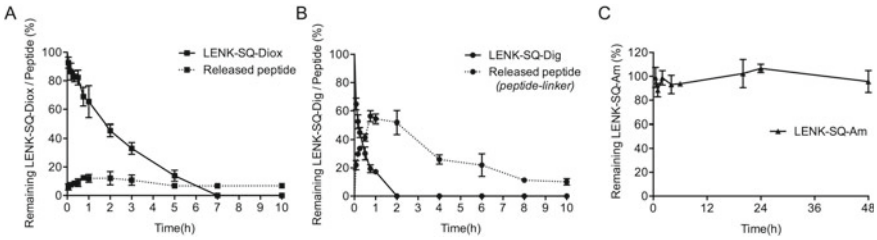

Fig. 6 In vitro bioconversion of LENK-SQ bioconjugates into LENK in the presence of serum. **A** LENK-SQ with dioxycarbonyl linker, **B** LENK-SQ with diglycolic linker, and **C** LENK-SQ with amide bond. Solid lines and dashed lines represent the bioconjugates and the released peptides, respectively. Figure reproduced from Ref. Feng et al. (2019), © 2019 AAAS

of a progressive release of the free LENK peptide which was subsequently slowly degraded by the peptidases of the serum, but still lasted beyond 10 h post-incubation (Fig. 6A). LENK-SQ-Dig NPs, for their part, decreased in serum until completely disappearance at 2 h, but no presence of free peptide was detected. Interestingly, the RP-HPLC analyses evidenced a slow release of the peptide still attached to its linker. The peptide-linker fragment reached a maximum at 45 min before undergoing progressive degradation but it could still be detected over 10 h (Fig. 6B). On the contrary, LENK-SQ-Am NPs remained stable in serum during 48 h, and no peptide was released thorough the experiment (Fig. 6C) (Feng et al. 2019). Interestingly, with the LENK-SQ-Diox bioconjugate, both the LENK and the SQ moieties were each attached to the dioxycarbonyl linker through an ester bond. In the case of the LENK-SQ-Dig bioconjugate, the diglycolate linker was linked on one side to SQ moiety through an ester bond while on the other side it was linked to the LENK through an amide bond. With regards to the LENK-SQ-Am bioconjugate, the LENK was directly connected to the SQ moiety through an amide bond. Given that generally amide bond is chemically and enzymatically more stable than ester bond, the absence of release of LENK from LENK-SQ-Am was not surprising (Simões et al. 2009; Wong and Choi 2015). Moreover, because LENK-SQ-Am and LENK-SQ-Dig are linear peptides, their N-terminal modification increased peptidase resistance (Oliyai 1996). Finally, as mouse serum is extremely rich in esterases, it is most likely that the release of LENK from LENK-SQ NPs was due to enzymatic hydrolysis of ester bond (Simões et al. 2009). Despite these *in vitro* data showing that depending on the type of linker, whether or not the LENK peptide was released, all the 3 bioconjugates were recruited for experimental algesimetry. It was expected that within the inflammation site, the more aggressive *in vivo* enzymatic medium, particularly rich in proteolytic enzymes, will contribute to the release of LENK from all the bioconjugates. Indeed, it was reported that the presence of high concentrations of proteolytic enzymes like chymotrypsin, cathepsin D and other proteases in inflammatory exudates play a crutial role in the inflammatory process (Viswanatha Swamy and Patil 2008).

7 Assessment of the Analgesic Activity of LENK-SQ NPs *in vivo*

The antinociceptive properties of LENK-SQ NPs were evaluated using a carrageenan-induced paw edema model in rats. The inflammation was generated by intraplantar injection of λ-carrageenan into the right hind paw thus inducing a local inflammatory response characterized by marked edema, hyperthermia, and hyperalgesia restricted to the injected right hind paw. Baseline measurements of paw withdrawal latencies (PWL) to a noxious thermal stimulus were first performed prior to carrageenan injection using Hargreaves test (Oliyai 1996) and presented a mean value ± SEM (n = 8) of 6.65 ± 0.37 s. Then, thermal sensitivities were evaluated 3 h after carrageenan injection, which corresponded to the peak inflammatory response, leading to a mean decrease of 52.48% of PWL compared to the basal PWLs in naïve rats (Fig. 8). Anti-hyperalgesic effects were assessed using the same test at various times during 4 h, after acute intravenous administration of the different drug treatments at this 3 h inflammation peak (Fig. 7). The acute treatment with morphine which was used as positive control (1 mg/kg), reduced the thermal hyperalgesia as shown by the resulting significant increase in PWLs. Indeed, the PWL reached 12.87 ± 1.38 s, 10 min after morphine injection, while it remained at 3.05 ± 0.20 s after treatment with a control dextrose solution (Fig. 8A). However, morphine analgesic activity disappeared rapidly and no longer significant effect was observed from 100 min post-morphine administration (Fig. 8A). Then, the anti-hyperalgesic effect of LENK-SQ NPs with the 3 different linkers was evaluated (Fig. 8C–H). All LENK-SQ NPs displayed a significant anti-hyperalgesic effect on inflamed hind paw leading to a significant reduction of thermal hyperalgesia, as expressed by a dramatic increase of respective AUC values in comparison with λ-carrageenan-treated rats injected with either the free LENK peptide or the blank SQ NPs (Fig. 8D, F, H). The anti-hyperalgesic effect was less intense than after morphine administration, but LENK-SQ NPs exhibited a much longer lasting effect. More specifically, the anti-hyperalgesic activity was notable during two hours from 10 to 130 min in rats injected with LENK-SQ Diox NPs or LENK-SQ Am NPs (Fig. 8C, G). Surprisingly, LENK-SQ-Am NPs, which were supposed to release the LENK slower than the two other NPs, have proved to be more potent but with a shorter duration, probably because the enzymatic capability in serum is not predictive of the enzymatic content in the inflamed paw. For their part, LENK-SQ-dig NPs also displayed a significant anti-hyperalgesic effect (Fig. 8E) which lasted twice as long as morphine. Indeed, LENK-SQ-dig NPs exhibited a maximum increase in PWL from 10 to 130 min post-injection, followed by a progressive decrease down to baseline at 220 min. It is interesting to note that the maximal PWL values corresponding to LENK-SQ NPs administration in λ-carrageenan-treated rats were comparable to basal PWL values measured in control naïve rats, before λ-carrageenan treatment (Fig. 8C, E, G), thus revealing a pure anti-hyperalgesic action of these NPs. However, the PWL values corresponding to the injection of morphine in λ-carrageenan-treated rats were twice

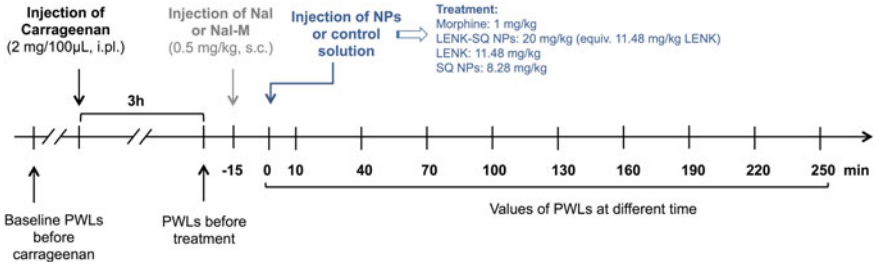

Fig. 7 Experimental design for algesimetry. The antinociceptive effect of NPs was tested in a pathophysiological context induced by an intraplantar carrageenan injection (2% saline, 100 µL). Involvement of central or peripheral opioid receptors was performed using a brain-permeant opioid antagonist, naloxone (Nal), and a brain-impermeant opioid receptor antagonist, naloxone methiodide (Nal-M). NP suspensions or control solutions were injected intravenously with a dose volume of 10 mL/kg during 30 s. The Hargreaves test was performed 10 min after the NP administration and then every 30 min up to a period of 250 min. The dose of LENK-SQ NPs (20 mg/kg) was equivalent to LENK (11.48 mg/kg) and to SQ NPs (8.28 mg/kg) and corresponded to 20.66 mmol/kg for both LENK-SQ and LENK. s.c., subcutaneous; i.pl., intraplantar. Figure reproduced from Ref. Feng et al. (2019), © 2019 AAAS

as high as those found in control naïve rats (Fig. 8A), which confirme the well established analgesic effect of the opiate agonist in addition to the anti-hyperalgesic effect. Furthermore, the absence of anti-hyperalgesic activity with blank SQ NPs (without the LENK) (Fig. 8), confirmed that the antinociceptive response to LENK-SQ NPs administration were due to the released LENK peptide. All these results seem to indicate that LENK-SQ NPs are particularly effective to treat hyperalgesia and are devoid of analgesic properties as with morphine. However, further studies are required to evaluate this hypothesis (Feng et al. 2019).

8 Effects of Opioid Receptor Blockade Using Naloxone and Naloxone Methiodide

For the purpose of establishing the involvement of central or peripheral opioid receptors during the anti-hyperalgesic effect of LENK-SQ NPs, opioid receptor antagonists such as naloxone (Nal, central and peripheral antagonist) or naloxone methiodide (Nal-M, peripheral antagonist) (Buller et al. 2005) were administered subcutaneously 15 min prior to the injection of NPs (Fig. 7). Pre-administration of either brain-permeant *Nal* or brain-impermeant Nal-M, abolished the anti-hyperalgesic effect of the three LENK-SQ NPs (Fig. 8C–H). Indeed, Nal pre-treatment resulted in a reduction of 66%, 105% or 73% of the AUC values compared to these found in rats injected with LENK-SQ-Diox, LENK-SQ-Dig and LENK-SQ-Am NPs alone, respectively. In the same way, pre-treatment with Nal-M caused a reduction of 81%, 99% and 96%, respectively, showing that the selective blockade of peripheral opioid receptors only

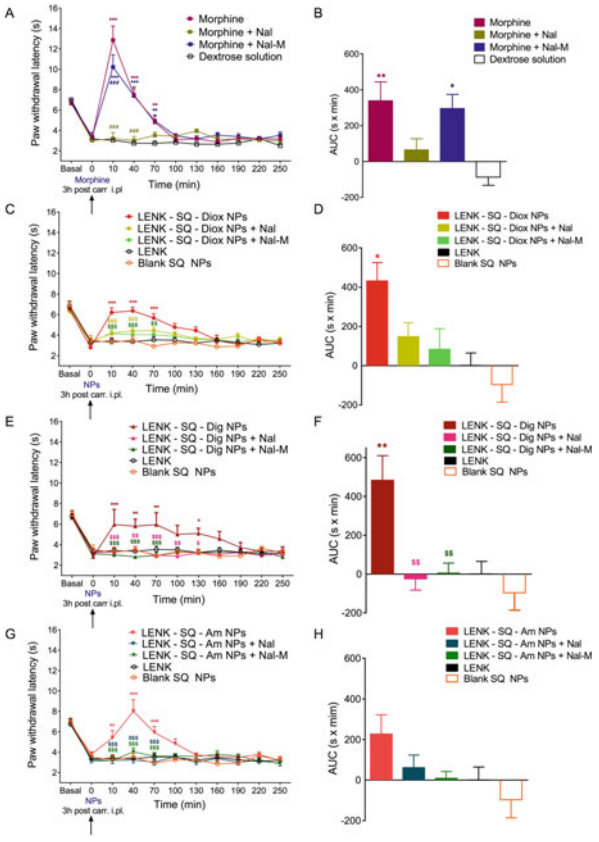

Fig. 8 Antihyperalgesic effect of LENK-SQ NPs and morphine. Antihyperalgesic effects of acute treatment with morphine **A** and **B**, LENK-SQ-Diox NPs **C** and **D**, LENK-SQ-Dig NPs **E** and **F**, and LENK-SQ-Am NPs **G** and **H** in λ-carrageenan–induced inflammatory pain injected rats. Administration of morphine, LENK-SQ NPs, Nal, Nal-M, LENK, blank SQ NPs, or dextrose solution (vehicle) was performed (arrows, 0 on abscissa) 3 h after λ-carrageenan injection into the right hind paw. Morphine (A), LENK-SQ-Diox NPs (C), LENK-SQ-Dig NPs (E), and LENK-SQ-Am NPs (G) induced an increase in PWL (in seconds, means ± SEM of independent determinations in five to nine animals per group) in the Hargreaves test. $^{*}P < 0.05$, $^{**}P < 0.01$, $^{***}P < 0.001$, compared to dextrose solution or LENK solution; $^{\#\#\#}P < 0.001$, compared to morphine; $^{\$}P < 0.05$, $^{\$\$}P < 0.01$, $^{\$\$\$}P < 0.001$, compared to LENK-SQ NPs. Two-way analysis of variance (ANOVA) with repeated measures, Bonferroni post test. Nal or Nal-M was administered 15 min before morphine or LENK-SQ NP injection. Basal on abscissa: Control (naïve) rats (before λ-carrageenan injection). (B, D, F, and H) Bars are the means ± SEM of AUCs (seconds × minutes) of the cumulative durations derived from the time course changes (A, C, E, and G) in PWL after the various treatments. $^{*}P < 0.05$, $^{**}P < 0.01$, $^{***}P < 0.001$, one-way ANOVA, Tukey post test, compared to dextrose (vehicle) or LENK solution; $^{\$}P < 0.05$, $^{\$\$}P < 0.01$, $^{\$\$\$}P < 0.001$, compared to LENK-SQ NPs. Two-way analysis of variance (ANOVA) with repeated measures, Bonferroni post test. Nal or Nal-M was administered 15 min before morphine or LENK-SQ NP injection. Basal on abscissa: Control (naïve) rats (before λ-carrageenan injection). (B, D, F, and H) Bars are the means ± SEM of AUCs (seconds × minutes) of the cumulative durations derived from the time course changes (A, C, E, and G) in PWL after the various treatments. $^{*}P < 0.05$, $^{**}P < 0.01$, $^{***}P < 0.001$, one-way ANOVA, Tukey post test, compared to dextrose (vehicle) or LENK solution; $^{\$}P < 0.05$, $^{\$\$} < 0.01$, $^{\$\$\$} < 0.001$, compared to LENK-SQ NPs Figure reproduced from Ref. Feng et al. (2019), © 2019 AAAS

was enough to abolish the anti-hyperalgesic effects of LENK-SQ NPs. It is interesting to note that in the case of morphine, pre-administration of Nal abrogated the amplitude and the duration of the anti-hyperalgesic effect of morphine in comparison with the morphine group while pre-treatment with Nal-M only marginally decreased the morphine's effect (by 13%) (Fig. 8A and B) showing that morphine acts mainly through central and, to a lesser extent, peripheral opioid receptors.

All these results clearly demonstrated that all three LENK-SQ NPs acted exclusively through peripherally located opioid receptors (Feng et al. 2019).

9 Biodistribution of LENK-SQ NPs

In order to investigate the ability of LENK-SQ NPs to address the neuropeptide towards the inflamed tissue, biodistribution studies were performed using *in vivo* fluorescence imaging. The *in vivo* biodistribution of LENK-SQ-Am NPs was assessed after intravenous injection of DiD-fluorescently labeled LENK-SQ-Am NPs in a murine λ-carrageenan-induced paw edema model (right hind paw). The fluorescence in tissues was tracked up to 24 h, non-invasively, from the abdomen side using an IVIS Lumina device (Fig. 9). After intravenous injection of fluorescent LENK-SQ-Am NPs, the real-time *in vivo* imaging showed a remarkable increase of fluorescence within the inflamed paw by 2–3 times of the average radiant efficiency in comparison with the healthy paw (Fig. 9A, D, F). In order to ensure that the accumulation of fluorescence in the λ-carrageenan-inflamed paw was not due to the local hind paw injection *per se*, normal mice were injected locally with saline in the hind paw and then intravenously treated with fluorescent LENK-SQ NPs (non-inflamed control). The absence of significant accumulation of fluorescence at hind paw level confirmed that the NPs accumulation is related to inflammation process induced by carrageenan (Fig. 9B, E). The intravenous injection of a single DiD solution (without NPs) in λ-carrageenan administered mice, didn't reveal, here again, significant accumulation of fluorescence in the inflamed paw (Fig. 9C, F).

With the aim of showing that the NPs reached intact the inflamed tissues, the LENK-SQ NPs containing two fluorescent probes, a the fluorescent DiD dye and a fluorescent DiR quencher, were incubated in serum. A progressive appearance of fluorescence indicated a relatively slow dissociation of the NPs in serum (20% after 5 min and 50% after 30 min) suggesting that under our *in vivo* conditions, a significant proportion of intact NPs could reach the inflamed tissues (Fig. 10).

Finally, in a separate experiment, the biodistribution of the fluorescence in different organs was performed. Thus, 4 h after the intravenous injection of fluorescent NPs or DiD solution, mice were euthanized and transcardially perfused with saline to eliminate the fluorescence which was in the blood circulation. The collected organs indicated a strong *ex vivo* fluorescence signal which was observed again in the inflamed paw, but also in the liver, the spleen and the lungs. Interestingly, no fluorescence was detected in the brain of the animals (Fig. 11) thus confirming that the anti-hyperalgesic effect resulted from the targeting of LENK-SQ NPs toward

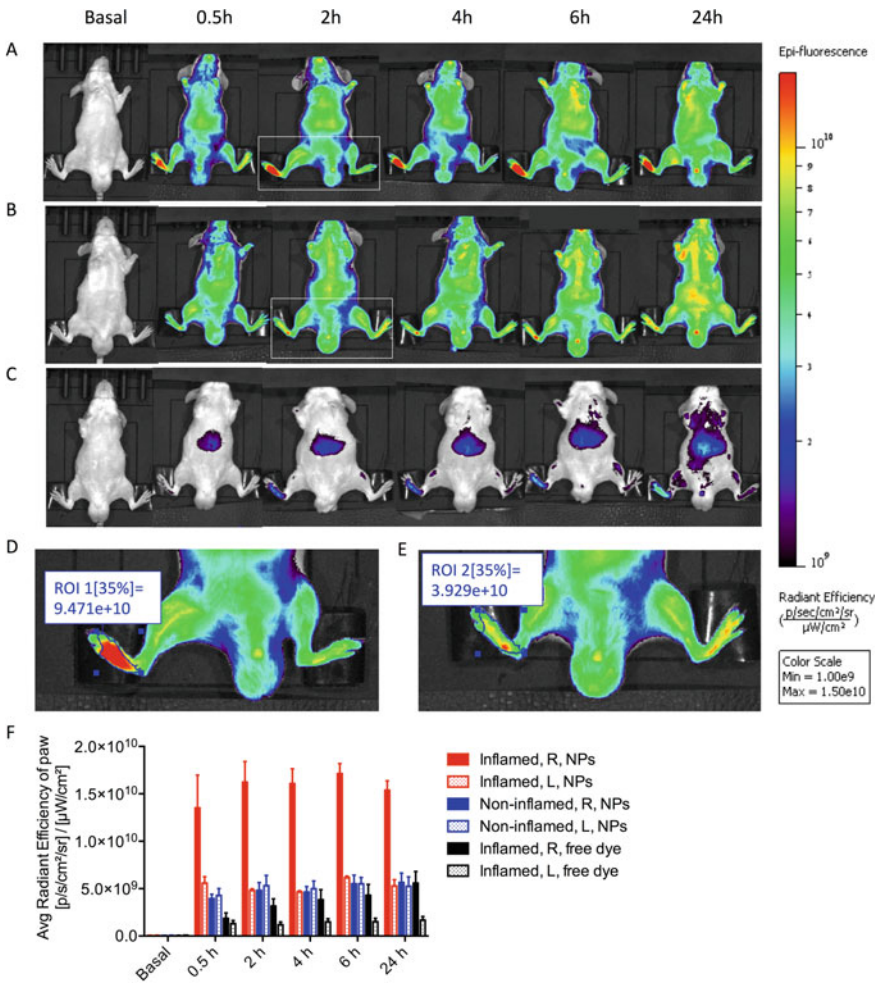

Fig. 9 IVIS Lumina scan of mice and of their organs after intravenous administration of fluorescent LENK-SQ-Am NPs or control fluorescent dye solution (ventral view). **A** Biodistribution of fluorescent LENK-SQ-Am NPs in mice with inflamed right hind paw. **B** Biodistribution of fluorescent LENK-SQ-Am NPs in mice with non-inflamed hind paw (saline injected only into the right hind paw). **C** Biodistribution of free dye in mice with inflamed right paw. **D** Zoom of group A at 2 h. **E**) Zoom of group B at 2 h. (**F**) Quantitative analysis of the paws with the same region of interest (ROI). R, right hind paw; L, left hind paw. Figure reproduced from Ref. Feng et al. (2019), © 2019 AAAS

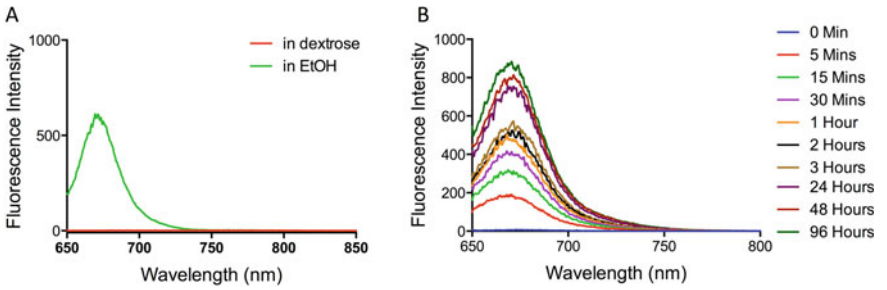

Fig. 10 In vitro colloidal stability of LENK-SQ-Am NPs in mouse serum. **A** Controls: When diluted in 5% dextrose LENK-SQ-Am NPs remained assembled (DiD: reporter dye; DiR: quencher). They disassembled in ethanol; **B** LENK-SQ-Am NPs (DiD: reporter dye; DiR: quencher) incubated in mouse serum (1:4). The fluorescence emission was measured to assess the progressive disassembly of the nanoparticles Figure reproduced from Ref. Feng et al. (2019), © 2019 AAAS

peripheral opioid receptors in inflamed tissue, rather than central opioid receptors (Feng et al. 2019).

10 Toxicity Study

Given that not negligible fluorescence was detected in some organs, indicating the potential presence of NPs in these tissues, the overall toxicity of LENK-SQ NPs was investigated 24 h and 48 h after their intravenous administration (20 mg/kg) in rats and compared to control animals injected with 5% dextrose solution. Concerning the liver, the levels of aspartate transaminase (AST) (Fig. 12A) and alanine transaminase (ALT) (Fig. 12B) were not increased in the LENK-SQ NPs group in comparison with control group, thus indicating no toxicity towards the liver. This was confirmed by histological analysis of this tissue at 24 h and 48 h (Fig. 12C–F). The histology of the spleen (Fig. 12G–J), the kidneys (Fig. 12K–N), the lungs (Fig. 12O–R) and the heart (Fig. 12S–V) didn't reveal any morphological anomaly after LENK-SQ NPs administration, too. All these results confirmed the safety of the LENK-SQ NPs upon systemic intravenous administration at the therapeutic dose of 20 mg/kg (Feng et al. 2019).

11 Conclusion

We describe here a novel nanomedicine approach based on the bioconjugation of endogenous LENK neuropeptide to biocompatible SQ, allowing the specific delivery of LENK for efficient pain control associated with inflammatory events. It was shown that LENK-SQ NPs exhibited an anti-hyperalgesic activity which lasted even longer

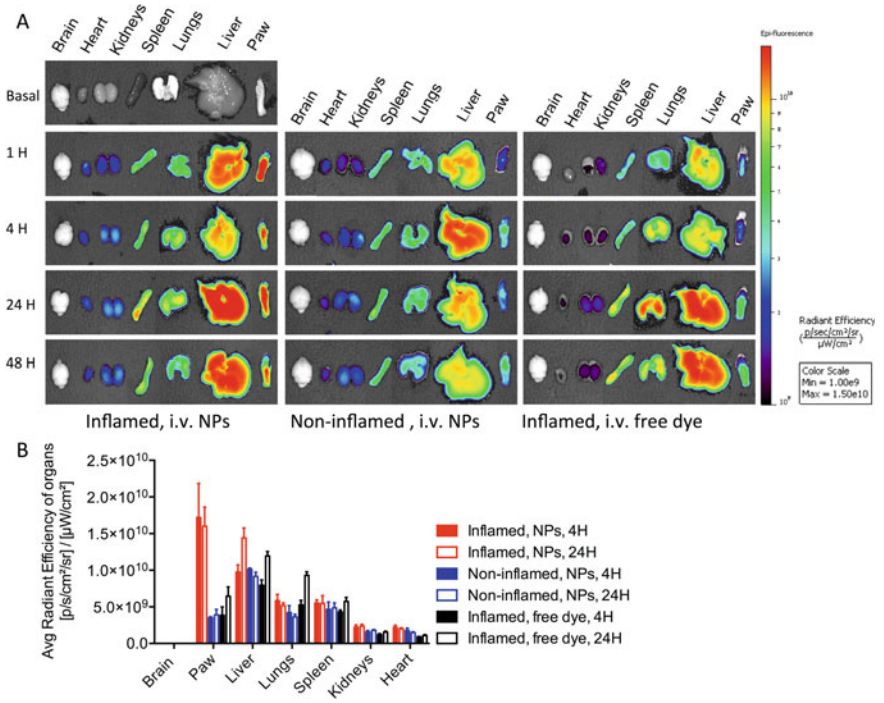

Fig. 11 Biodistribution of fluorescent LENK-SQ-Am NPs or control fluorescent dye solution in mice with or without inflamed paw. 4 h after λ-carrageenan or saline injection into the right paw, fluorescent LENK-SQ NPs or free dye were intravenously introduced into the mice. At different time points, mice were deeply anesthetized with a mixture of ketamine (100 mg/kg, i.p.) and xylazine (10 mg/kg, i.p.) before euthanasia by transcardiac perfusion of 40 ml saline (8 mL/min), until the fluid exiting the right atrium was entirely clear. Then, liver, spleen, kidneys, heart, lungs, brain, and inflamed right hind paw were excised and immediately imaged with the imager. The fluorescence emitted was quantified with Living Image software over the region of interest (ROI) with the threshold of 20%. (A) Ex vivo fluorescence imaging of the harvested brain, heart, kidneys, lungs, liver and paw from fluorescent NPs or free dye-injected SWISS mice. (B) Average radiant efficiency of these organs after 4 or 24 h injection of NPs or free dye. Figure reproduced from Ref. Feng et al. (2019), © 2019 AAAS

than with morphine, by activation of peripherally located opioid receptors. The experimental approach to prepare these NPs is simple, safe and easy, which should facilitate further pharmaceutical development and clinical translation. Although further studies are needed to more precisely determine how the pharmacodynamics of LENK-SQ NPs may affect the clinical outcome, this study opens a new exciting perspective for an efficient treatment of intense pain, devoid of severe side effects associated with morphine or related synthetic opioids.

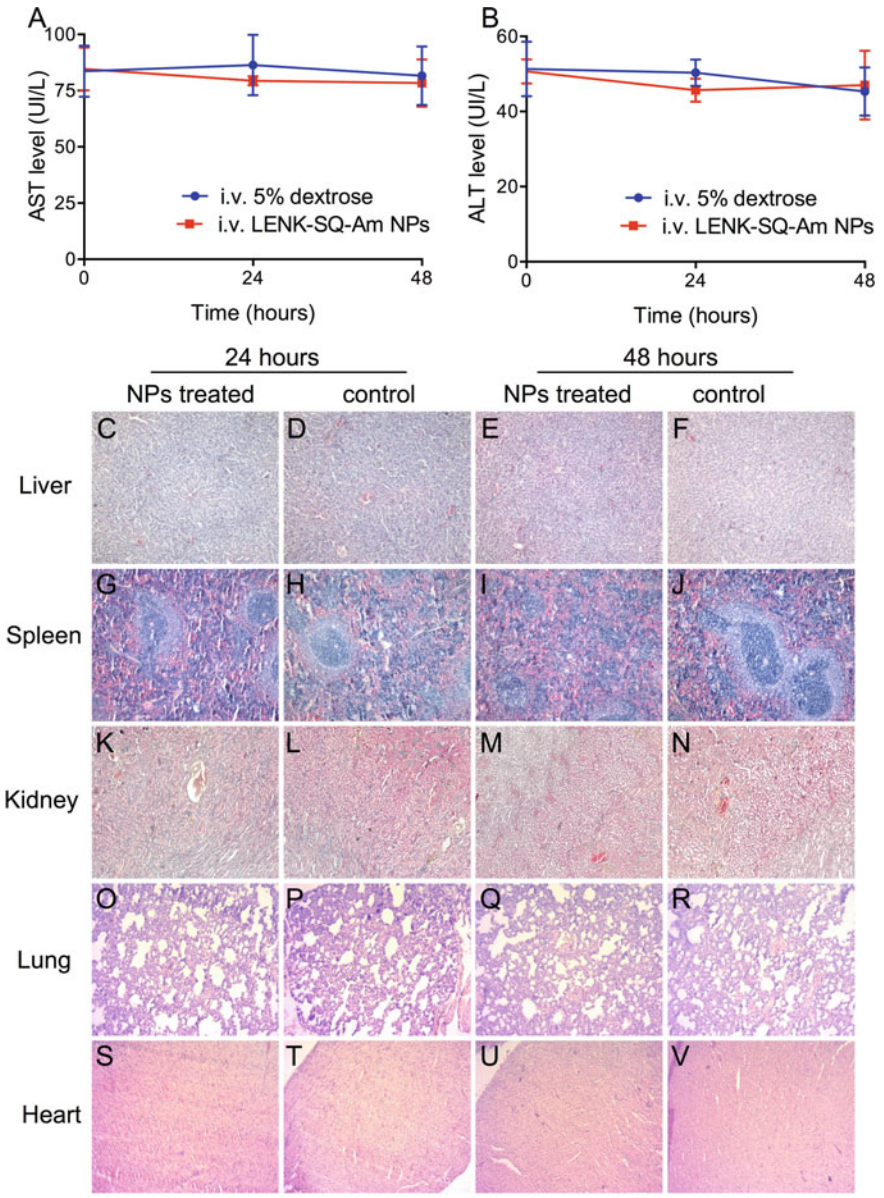

Fig. 12 Toxicity study of LENK-SQ-Am NPs upon systemic administration. LENK-SQ-Am NPs (20 mg/kg) were intravenously administered in rats. The AST (A) and ALT (B) levels in plasma showed no differences compared with dextrose solution (data presented as mean UI/L ± SED, N = 3 animals per group). Histological analysis of organs after intravenous administration of LENK-SQ-Am NPs (20 mg/kg) did not show any signs of cell or tissue damage at 24 h and 48 h, comparatively to a control 5% dextrose solution. Liver (C-F), spleen (G-J), kidneys (K-N), lungs (O-R) and heart (S-V). All tissue images were analyzed by microscopy at 10× magnification except for kidneys which were at 5 × magnification (Zeiss). Figure reproduced from Ref. Feng et al. (2019), © 2019 AAAS

References

Abbadie C, Abbadie GW (2002) Endorphins and their receptors. In: Encyclopedia of the human brain. Elsevier (2002), pp 193–200. https://doi.org/10.1016/B0-12-227210-2/00137-0

Adams JM (2018) Increasing naloxone awareness and use: the role of health care practitioners. JAMA 319(20):2073. https://doi.org/10.1001/jama.2018.4867

Adams D, Gonzalez-Duarte A, O'Riordan WD, Yang C-C, Ueda M, Kristen AV, Tournev I, Schmidt HH, Coelho T, Berk JL, Lin K-P, Vita G, Attarian S, Planté-Bordeneuve V, Mezei MM, Campistol JM, Buades J, Brannagan TH, Kim BJ, Oh J, Parman Y, Sekijima Y, Hawkins PN, Solomon SD, Polydefkis M, Dyck PJ, Gandhi PJ, Goyal S, Chen J, Strahs AL, Nochur SV, Sweetser MT, Garg PP, Vaishnaw AK, Gollob JA, Suhr OB (2018) Patisiran, an RNAi therapeutic, for hereditary transthyretin amyloidosis. N Engl J Med 379(1):11–21. https://doi.org/10.1056/NEJMoa1716153

Anselmo AC, Mitragotri S (2016) Nanoparticles in the clinic: nanoparticles in the clinic. Bioeng Transl Med 1(1):10–29. https://doi.org/10.1002/btm2.10003

Bobo D, Robinson KJ, Islam J, Thurecht KJ, Corrie SR (2016) Nanoparticle-based medicines: a review of FDA-approved materials and clinical trials to date. Pharm Res 33(10):2373–2387. https://doi.org/10.1007/s11095-016-1958-5

Barenholz Y (Chezy). Doxil® — The first FDA-approved nano-drug: lessons learned. J Control Release **2012**, 160(2): 117–134. https://doi.org/10.1016/j.jconrel.2012.03.020

Betageri GV, Vutla NB, Banga AK (1997) Liposomal formulation and characterization of the opioid peptide leucine enkephalin. Pharm Sci 3:587–591. https://doi.org/10.1111/j.2042-7158.1997.tb00502.x

Bonvalot S, Rutkowski PL, Thariat J, Carrère S, Ducassou A, Sunyach M-P, Agoston P, Hong A, Mervoyer A, Rastrelli M, Moreno V, Li RK, Tiangco B, Herraez AC, Gronchi A, Mangel L, Sy-Ortin T, Hohenberger P, de Baère T, Le Cesne A, Helfre S, Saada-Bouzid E, Borkowska A, Anghel R, Co A, Gebhart M, Kantor G, Montero A, Loong HH, Vergés R, Lapeire L, Dema S, Kacso G, Austen L, Moureau-Zabotto L, Servois V, Wardelmann E, Terrier P, Lazar AJ, Bovée, JVMG, Le Péchoux C, Papai Z (2019) NBTXR3, a first-in-class radioenhancer hafnium oxide nanoparticle, plus radiotherapy versus radiotherapy alone in patients with locally advanced soft-tissue sarcoma (Act.In.Sarc): a multicentre, phase 2–3, randomised, controlled trial. Lancet Oncol 20(8):1148–1159. https://doi.org/10.1016/S1470-2045(19)30326-2

Buller K, Hamlin A, Osborne P (2005) Dissection of peripheral and central endogenous opioid modulation of systemic interleukin-1β responses using c- expression in the rat brain. Neuropharmacology 49(2):230–242. https://doi.org/10.1016/j.neuropharm.2005.03.014

Büscher HH, Hill RC, Römer D, Cardinaux F, Closse A, Hauser D, Pless J (1976) Evidence for analgesic activity of enkephalin in the mouse. Nature 261(5559):423–425. https://doi.org/10.1038/261423a0

Carnevale J, Ko AH (2016) MM-398 (nanoliposomal irinotecan): emergence of a novel therapy for the treatment of advanced pancreatic cancer. Future Oncol 12(4):453–464. https://doi.org/10.2217/fon.15.333

Chang TC, Shiah HS, Yang CH, Yeh KH, Cheng AL, Shen BN, Wang YW, Yeh CG, Chiang NJ, Chang JY, Chen LT (2015) Phase I study of nanoliposomal irinotecan (PEP02) in advanced solid tumor patients. Cancer Chemother Pharmacol 75(3):579–586. https://doi.org/10.1007/s00280-014-2671-x

Chen Y, Wang F, Benson HAE (2008) Effect of formulation factors on incorporation of the hydrophilic peptide dalargin into PLGA and MPEG-PLGA nanoparticles. Biopolymers 90(5):644–650. https://doi.org/10.1002/bip.21013

Contet C, Kieffer BL, Befort K (2004) Mu opioid receptor: a gateway to drug addiction. Curr Opin Neurobiol 14(3):370–378. https://doi.org/10.1016/j.conb.2004.05.005

Couvreur P, Stella B, Reddy LH, Hillaireau H, Dubernet C, Desmaële D, Lepêtre-Mouelhi S, Rocco F, Dereuddre-Bosquet N, Clayette P, Rosilio V, Marsaud V, Renoir J-M, Cattel L (2006) Squalenoyl nanomedicines as potential therapeutics. Nano Lett 6(11):2544–2548. https://doi.org/10.1021/nl061942q

Coyne DW, Auerbach M (2010) Anemia management in chronic kidney disease: intravenous iron steps forward. Am J Hematol NA-NA. https://doi.org/10.1002/ajh.21682

Cummings GC, Dixon J, Kay NH, Windsor JPW, Major E, Morgan M, Sear JW, Spence AA, Stephenson DK (1984) Dose requirements of ICI 35,868 (propofol, 'Diprivan') in a new formulation for induction of anaesthesia. Anaesthesia 39(12):1168–1171. https://doi.org/10.1111/j.1365-2044.1984.tb06425.x

Desmaële D, Gref R, Couvreur P (2012) Squalenoylation: a generic platform for nanoparticular drug delivery. J Control Release 161(2):609–618. https://doi.org/10.1016/j.jconrel.2011.07.038

Dykstra L, Granger AL, Allen RM, Zhang X, Rice KC (2002) Antinociceptive effects of the selective delta opioid agonist SNC80 alone and in combination with mu opioids in the squirrel monkey titration procedure. Psychopharmacology 163(3–4):420–429. https://doi.org/10.1007/s00213-002-1100-8

Fan Y, Marioli M, Zhang K (2021) Analytical characterization of liposomes and other lipid nanoparticles for drug delivery. J Pharm Biomed Anal 192:113642. https://doi.org/10.1016/j.jpba.2020.113642

Feng J, Lepetre-Mouelhi S, Couvreur P (2017) Design, preparation and characterization of modular SQ-based nanosystems for controlled drug release. CTMC 17(25). https://doi.org/10.2174/1568026617666170719171728

Feng J, Lepetre-Mouelhi S, Gautier A, Mura S, Cailleau C, Coudore F, Hamon M, Couvreur P (2019) A new painkiller nanomedicine to bypass the blood-brain barrier and the use of morphine. Sci Adv 5(2), eaau5148. https://doi.org/10.1126/sciadv.aau5148

Fox JL (1995) FDA advisors okay NeXstar's DaunoXome. Nat Biotechnol 13(7):635–636. https://doi.org/10.1038/nbt0795-635

Gupta AK, Gupta M (2005) Synthesis and surface engineering of iron oxide nanoparticles for biomedical applications. Biomaterials 26(18):3995–4021. https://doi.org/10.1016/j.biomaterials.2004.10.012

Gylling H, Miettinen TA (1994) Postabsorptive metabolism of dietary SQ. Atherosclerosis 106(2):169–178. https://doi.org/10.1016/0021-9150(94)90122-8

Hamill RJ (2013) Amphotericin B formulations: a comparative review of efficacy and toxicity. Drugs 73(9):919–934. https://doi.org/10.1007/s40265-013-0069-4

Jackson LA, Anderson EJ, Rouphael NG, Roberts PC, Makhene M, Coler RN, McCullough MP, Chappell JD, Denison MR, Stevens LJ, Pruijssers AJ, McDermott A, Flach B, Doria-Rose NA, Corbett KS, Morabito KM, O'Dell S, Schmidt SD, Swanson PA, Padilla M, Mascola JR, Neuzil KM, Bennett H, Sun W, Peters E, Makowski M, Albert J, Cross K, Buchanan W, Pikaart-Tautges R, Ledgerwood JE, Graham BS, Beigel JH (2020) An MRNA vaccine against SARS-CoV-2 — preliminary report. N Engl J Med 383(20):1920–1931. https://doi.org/10.1056/NEJMoa2022483

Janecka A, Fichna J, Janecki T (2004) Opioid receptors and their ligands. CTMC 4(1):1–17. https://doi.org/10.2174/1568026043451618

Kiritsy-Roy JA, Marson L, Van Loon GR (1989) Sympathoadrenal, cardiovascular and blood gas responses to highly selective mu and delta opioid peptides. J Pharmacol Exp Ther 251(3):1096–1103

Krauss AC, Gao X, Li L, Manning ML, Patel P, Fu W, Janoria KG, Gieser G, Bateman DA, Przepiorka D, Shen YL, Shord SS, Sheth CM, Banerjee A, Liu J, Goldberg KB, Farrell AT, Blumenthal GM, Pazdur R (2019) FDA approval summary: (daunorubicin and cytarabine) liposome for injection for the treatment of adults with high-risk acute myeloid leukemia. Clin Cancer Res 25(9):2685–2690. https://doi.org/10.1158/1078-0432.CCR-18-2990

Laurent S, Forge D, Port M, Roch A, Robic C, Vander Elst L, Muller RN (2008) Magnetic iron oxide nanoparticles: synthesis, stabilization, vectorization, physicochemical characterizations, and biological applications. Chem. Rev. 108(6):2064–2110. https://doi.org/10.1021/cr068445e

Leonard RCF, Williams S, Tulpule A, Levine AM, Oliveros S (2009) Improving the therapeutic index of anthracycline chemotherapy: focus on liposomal doxorubicin (Myocet^{TM}). Breast 18(4):218–224. https://doi.org/10.1016/j.breast.2009.05.004

Maeda H (2012) Macromolecular therapeutics in cancer treatment: the EPR effect and beyond. J Control Release 164(2):138–144. https://doi.org/10.1016/j.jconrel.2012.04.038

Mandal PK, McMurray JS (2007) Pd−C-induced catalytic transfer hydrogenation with triethylsilane. J. Org. Chem. 72(17):6599–6601. https://doi.org/10.1021/jo0706123

Miettinen TA, Vanhanen H (1994) Serum concentration and metabolism of cholesterol during rapeseed oil and SQ feeding. Am J Clin Nutr 59(2):356–363. https://doi.org/10.1093/ajcn/59.2.356

Na HB, Song IC, Hyeon T (2009) Inorganic nanoparticles for MRI contrast agents. Adv Mater 21(21):2133–2148. https://doi.org/10.1002/adma.200802366

Oliyai R (1996) Prodrugs of peptides and peptidomimetics for improved formulation and delivery. Adv Drug Deliv Rev 19(2):275–286. https://doi.org/10.1016/0169-409X(95)00110-S

Pasternak GW, Abbadie C (2013) Opioid receptor localization. In: Gebhart GF, Schmidt RF (eds) Encyclopedia of pain. Springer, Heidelberg, pp 2436–2441. https://doi.org/10.1007/978-3-642-28753-4_2961

Peer D, Karp JM, Hong S, Farokhzad OC, Margalit R, Langer R (2007) Nanocarriers as an emerging platform for cancer therapy. Nature Nanotech 2(12):751–760. https://doi.org/10.1038/nnano.2007.387

Rust DM, Jameson G (1998) The novel lipid delivery system of amphotericin B: drug profile and relevance to clinical practice. Oncol Nurs Forum 25(1):35–48

Schmidt-Erfurth U, Hasan T (2000) Mechanisms of action of photodynamic therapy with verteporfin for the treatment of age-related macular degeneration. Surv Ophthalmol 45(3):195–214. https://doi.org/10.1016/S0039-6257(00)00158-2

Sémiramoth N, Meo CD, Zouhiri F, Saïd-Hassane F, Valetti S, Gorges R, Nicolas V, Poupaert JH, Chollet-Martin S, Desmaële D, Gref R, Couvreur P (2012) Self-assembled squalenoylated penicillin bioconjugates: an original approach for the treatment of intracellular infections. ACS Nano 6(5):3820–3831. https://doi.org/10.1021/nn204928v

Silverman JA, Deitcher SR (2013) Marqibo® (vincristine sulfate liposome injection) improves the pharmacokinetics and pharmacodynamics of vincristine. Cancer Chemother Pharmacol 71(3):555–564. https://doi.org/10.1007/s00280-012-2042-4

Simões MF, Valente E, Gómez MJR, Anes E, Constantino L (2009) Lipophilic pyrazinoic acid amide and ester prodrugs. Eur J Pharm Sci 37(3–4):257–263. https://doi.org/10.1016/j.ejps.2009.02.012

Tavani A, Petrillo P, La Regina A, Sbacchi M (1990) Role of peripheral mu, delta and kappa opioid receptors in opioid-induced inhibition of gastrointestinal transit in rats. J Pharmacol Exp Ther 254(1):91–97

Thompson KA, Goodale DB (2000) The recent development of propofol (DIPRIVAN®). Intensive Care Med 26(S3):S400–S404. https://doi.org/10.1007/PL00003783

Tomao, S (2009) Albumin-bound formulation of paclitaxel (Abraxane® ABI-007) in the treatment of breast cancer. IJN 99. https://doi.org/10.2147/IJN.S3061

Viswanatha Swamy AHM, Patil P (2008) Effect of some clinically used proteolytic enzymes on inflammation in rats. Indian J Pharm Sci 70(1):114. https://doi.org/10.4103/0250-474X.40347

Wang Y-XJ, Hussain SM, Krestin GP (2001) Superparamagnetic iron oxide contrast agents: physicochemical characteristics and applications in MR imaging. Eur Radiol 11(11):2319–2331. https://doi.org/10.1007/s003300100908

Wang AZ, Langer R, Farokhzad OC (2012) Nanoparticle delivery of cancer drugs. Annu Rev Med 63(1):185–198. https://doi.org/10.1146/annurev-med-040210-162544

Wong PT, Choi SK (2015) Mechanisms of drug release in nanotherapeutic delivery systems. Chem Rev 115(9):3388–3432. https://doi.org/10.1021/cr5004634